PAPER

Flexible wide-range capacitive pressure sensor using micropore PE tape as template

IOP Publishing Smart Materials and Structures
Smart Mater. Struct. **28** (2019) 115040 (8pp) https://doi.org/10.1088/1361-665X/ab4ac6

Flexible wide-range capacitive pressure sensor using micropore PE tape as template

Qiang Zhang[1], Wendan Jia[1], Chao Ji, Zhen Pei, Zhu Jing, Yongqiang Cheng, Wendong Zhang, Kai Zhuo, Jianlong Ji, Zhongyun Yuan and Shengbo Sang

Micro Nano System Research Center, Key Lab of Advanced Transducers and Intelligent Control System of the Ministry of Education & College of Information and Computer, Taiyuan University of Technology, Taiyuan, 030024, People's Republic of China

E-mail: sunboa-sang@tyut.edu.cn

Received 17 June 2019, revised 26 August 2019
Accepted for publication 3 October 2019
Published 22 October 2019

Abstract

Flexible pressure sensors based on capacitive induction have become a research hot-spot because of low energy consumption and excellent performance in recent years. In practical applications, a wide range of detection and low-cost mass-produced flexible pressure sensors are ideal. Herein, this paper presents a wide detection range capacitive pressure sensor based on a structured elastic electrode, which is low cost and can be mass-produced by a simple method of micropore PE tape molding. Test results show that the sensor's pressure detection range is 0–45 kPa. This is because the upper structure of the capacitive sensor is constantly changing when subjected to different external pressures, so that the contact area of the upper substrate of the sensor becomes larger and the distance between the upper and lower substrates becomes smaller. In addition, this capacitive pressure sensor exhibits low detection limit (<300 Pa), ultra-short response time (<50 ms) and high operational stability for repeated loading/unloading pressure cycles. The sensor owns excellent resolution and can distinguish language, and the sensor can be used to monitor pulse. Low-cost mass production and wide detection range of flexible capacitive pressure sensors lay the foundation for the development of electronic skin, contact inspection applications and wearable healthcare monitors.

Keywords: Ag@CNTs, silver nanowires, structured flexible pressure sensor, capacitive sensor

(Some figures may appear in colour only in the online journal)

1. Introduction

Recently, there has been an ever growing demand for large area and stretchable pressure sensors due to their potential applications in wearable electronic devices such as electronic skin [1–5], robotic skin [6–8], biomedical diagnostics [9–11] and healthcare monitors [12–16]. The flexible pressure sensors with high mechanical flexibility and high sensitivity are quite required so as to achieve the above technology [17]. Based on the sensing mechanism, the pressure sensors are divided into piezoresistive [18–22], piezocapacitive [23–27], piezoelectric [28–31] and triboelectric pressure sensors [32, 33]. Among them, the flexible pressure sensors based on capacitive induction have the advantages of short response time, low detection limit and high working stability [34–37]. Thence, capacitive sensitive pressure sensors have recently become a research hot-spot.

Pressure sensitivity, detection limits, response time and operational stability are the most vital characteristics of the four pressure sensors [38, 39]. In order to improve the performance of the sensors, we need to consider the two aspects of material selection and sensor structure [40, 41]. So far, active materials used as tactile sensors include carbon nanotubes (CNTs), graphene, conductive polymers, metal, semiconductor nanowires and so on [38, 39]. Among these numerous nanomaterials, silver nanowire (AgNWs) are widely used in flexible pressure sensors for their excellent electrical properties. Shuai *et al* prepared a capacitive pressure

[1] These authors contributed equally to this work.

sensor with high sensitivity (2.94 kpa^{-1}) using polyvinylidene fluoride (PVDF) film as the dielectric layer, AgNWs coating as the top electrode and polydimethylsiloxane (PDMS) as the substrate [17]. In order to improve the sensitivity and sensing range of flexible pressure sensors, CNTs are also increasingly applied in flexible pressure sensors due to the advantages such as low cost, small size, fiber structure, good electrical and mechanical properties [38]. For instance, Zhou *et al* developed a 'skeletal' mechanical sensor with sensitivity of 10^5 MPa^{-1}, pressure of 0.9 MPa and pressure range of 0–1.5 MPa by embedding low-strength wet-spun single-walled CNT wires in PDMS. Among them, CNTs are used as a functional material to improve the performance of the device [42]. Therefore, by combining silver nanoparticles and CNTs into a composite nanomaterial, the excellent performance of each of the silver nanomaterial and the CNTs can be more fully exerted, and the effect of the Ag–C composite material is greatly improved [43–45]. In our previous work, the flexible strain sensor based on Ag@CNT nanomaterials has been studied. The pore structure and excellent conductivity of the nanocomposites were determined [44]. In addition, in order to improve the performance of the sensor, many sensors usually use some special surface structure design. The active electrode is largely deformed by applying external pressure and a large number of convex structures increase the surface contact roughness, so that the sensor exhibits higher sensitivity and wider detection limit [38, 39, 46, 47]. Wang *et al* reported an ultra-high sensitivity (1.8 kpa^{-1}) sensor using a low-cost silk fabric molding method [46]. Li *et al* reported a flexible capacitive tactile sensor with high sensitivity (0.815 kpa^{-1}) based on the utilization of bionic microstructures molded by natural lotus leaves [47]. This indicates that the presence of microstructures improves the performance of the sensor. Therefore, the existence of structures are necessary in the design of the sensor and finding templates that are not easily deformed and broken during the molding process has become a hot focus of attention.

Hence, based on our previous research about the Ag@CNTs nanomaterials with pore structure and excellent conductivity, this paper uses this material as the upper substrate sensitive electrode material. The micropore PE tape is used with fixed structure as the template because it is an item that is available in our lives and is low in cost. We use a special method to embed Ag@CNTs into PDMS for molding. The micropore PE tape will not be deformed when the substrate is warmed and the tape is peeled off without causing damage to the substrate. In order to verify that the upper substrate molded by the micropore PE tape has a structure, the surface and cross section of the molded upper substrate were characterized by scanning electron microscope (SEM) in this paper. Then, the sensors of different electrode structures and different dielectric layers were compared and tested as well. It comes to a conclusion that the nanomaterials with pore structure and the microstructure of the upper substrate both help widen the sensing range of the flexible pressure sensor. Based on the experimental results, we selected a stable and excellent sensor for application tests. Through a series of stress tests, the sensor is functionally analyzed and tested to obtain the flexible tactile sensor for pressure testing applications. For instance, the movement state of the throat vibration when the sound is emitted by the change of the output curve of the sensor can be judged, the language we speak can be detected, and even the vibration of the pulse can be monitored.

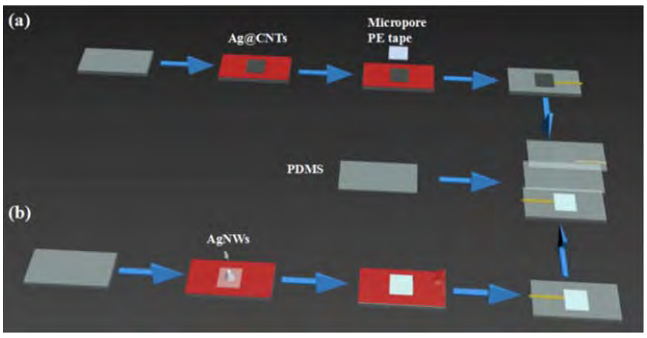

Figure 1. Manufacturing process of capacitive tactile sensor.

2. Experiment

2.1. Materials

The materials used in the synthesis of AgNWs are glycol solution (EG, 99.5%), polyvinylpyrrolidone (PVP), ferric chloride ($FeCl_3$, 99.5%), potassium bromide (KBr, 99.0%) and silver nitrate ($AgNO_3$, 99.0%). The materials used in the synthesis of Ag@CNTs are silver nitrate aqueous solution (AR, 0.26 mM), MWCNTs (Hydroxylated multi-walled CNTs, >95 wt%, –COOH content: 2.56 wt%, inner diameter: 3–5 nm, outer diameter: 8–15 nm, length: 50 μm, resistivity: 100 s cm^{-1}), sodium citrate aqueous solution (AR, 1 wt%). PDMS elastomer was purchased from Dow Corning, Sylgard 184. Micropore PE tape purchased from KeFu, PE tape.

Synthesis of AgNWs: Pour 100 ml solution of ethylene glycol into a round-bottomed flask and leave for 1 h at 160 °C. Then pour 700 μl of $FeCl_3$ aqueous solution into the flask and stir the aqueous solution for 15 min. Then drop 5 ml PVP solution and 5 ml $AgNO_3$ aqueous solution successively into the flask. After 1 h, the obtained solution was ice-cooled. Finally, the sample was washed with ethanol after centrifugation (10 000 rpm/rct) [45].

Synthesis of Ag@CNT: Place a flask of aqueous 15 ml silver nitrate on a magnetic stirrer and heat it to 100 °C. Then, 2 mg MWCNTs and 20 ml sodium citrate aqueous solution were successively added into the flask. After stirring at 100 °C for 30 min, the solution turned to gray. The sample of Ag@CNTs was obtained after centrifugation at 10 000 rpm/rct via centrifuge [43, 44].

2.2. Fabrication of the capacitive pressure sensor

The detailed fabrication process for making a capacitive pressure sensor is shown in figure 1. The production process is divided into the upper, middle and lower parts of figure 1.

Among them, the middle part is the dielectric PDMS required to make the capacitive pressure sensor, and the section height is 0.5 mm. Figure 1(a) is the manufacturing process of the upper substrate. As shown in the figure, the PDMS of a certain size was placed on a constant temperature heating box (XG-2020) and heated at 70 °C for 15 min, then the cut insulating tape was pasted on the PDMS which in a semi-dry state. (A square of size 1 × 1 cm^2 was cut in the middle of the red insulating tape as shown.) Then spread the prepared and ground Ag@CNTs in the middle of the tape, cover the structured side of the micropore PE tape on the Ag@CNTs, and continue heating on the hot plate until the PDMS was completely dry. Finally the micropore PE tape and the insulating tape were removed, and drew the copper wire on the side of the substrate with the special structure as the upper electrode to complete the fabrication of the upper substrate. The lower part is the manufacturing process of the lower substrate. As shown in the figure 1(b), the PDMS of a certain size was also placed on a hot plate at 70 °C for 30 min and the insulating tape cut as described above was pasted, and then AgNWs were evenly spread. (The preparation methods of AgNWs and Ag@CNTs were reported in the preliminary works [43–45].) The insulating tape was removed after the AgNWs were dried, and the copper wire was taken out on one side to complete the fabrication of the lower substrate. Finally, these three parts were packaged to complete the manufacture of a special structure capacitive pressure sensor.

2.3. Characterization and measurement

The sample was obtained after centrifugation via centrifuge (Eppendorf Centrifuge 5804, Hunan, China). The solution is heated by a magnetic stirrer (JOANLAB, HSC-19T). The micro-structure of the sample was identified by a field emission SEM (JEOL-7100F). The uniform PDMS film was made by the spin coater (Analysis EZ4). The PDMS was heated with a constant temperature heating station (XG-2020). The pressure sensor was fixed on the pressure tester (ZHIQU), and the pressure tester was used to control the pressure applied to the sensor. The two copper wires on the sensor were connect to the capacitance tester (GWINSTEK, LCR-8110G) and the capacitance of the pressure sensor changes with the applied pressure was measured.

3. Results and discussion

The surface micro-structure of the micropore PE tape and the top electrode molded by the micropore PE tape was characterized by SEM, as shown in figure 2. For micropore PE tape, it can be seen in figure 2(a). The main picture shows an SEM image of the micropore PE tape with special structure. It can be seen from the figure that it has an obvious and distinguishable regular shape. The illustration is the optical photo of the micropore PE tape used. Figure 2(b) is an SEM image of PDMS molded with micropore PE tape (five special complete structures are shown). This indicates that the shape of micropore PE tape has been molded and printed on the

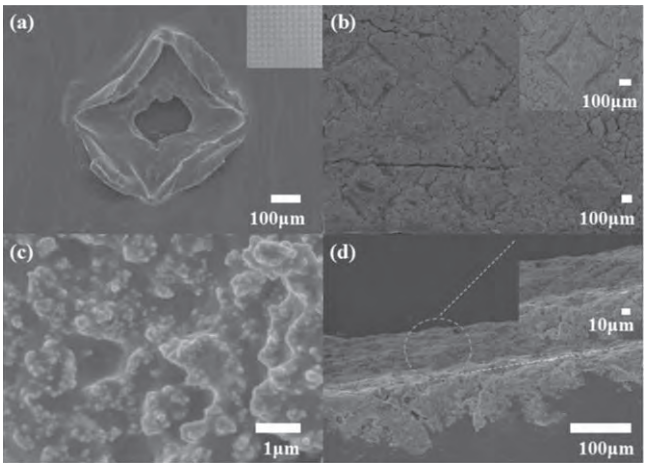

Figure 2. (a) SEM image of a single structure of micropore PE tape, illustration is an optical photo of micropore PE tape. (b) SEM image and illustration of a part of the enlarged image after molding with micropore PE tape. (c) SEM image of Ag@CNTs material after molding of micropore PE tape. (d) SEM cross section of the upper plate with special structure after molding of micropore PE tape and a part of enlarged view thereof.

PDMS and can be completely molded on the upper substrate. The illustration is a magnified view of a particular structure. By comparing figure 2(a), it can be found that the shapes and the sizes are the same. Figure 2(c) is a SEM observation of the material Ag@CNTs after molding the micropore PE tape. It can be seen from the figure that Ag nanoparticles are coated around the CNTs. Figure 2(d) is an SEM image of a cross section of an upper substrate having a special structure after molding of a micropore PE tape, and an SEM cross-sectional view of an enlarged portion thereof. It can be observed that Ag@CNTs are embedded in PDMS and obvious concavo-convex structure can be seen on the surface, which indicates that it is effective to use a micropore PE tape having a regular structure as a template.

According to the above introduction and on the basis of this, the structured pressure sensors are designed. The existence of a large number of concave-convex structures greatly increases the surface roughness of the electrode and provides rich contact cites for realizing high sensitivity pressure sensors. On the one hand, the active electrode undergoes larger deformation and the contact point with the medium increases when external pressure is applied. On the other hand, as the pressure increases, distance changes caused by gap shrinkage between the upper and lower layers of the electrode can greatly affect the capacitance. These both can lead to higher sensitivity and wider detection limit for piezocapacitive sensors, thereby improving the performance of the sensor [48]. Therefore, the microstructure of the electrode has a great effect on the performance of the pressure sensor in principle. In order to verify this, we have produced four different piezocapacitive sensors, which compare the capacitance characteristics of piezocapacitive sensors of different media and the capacitance characteristics of piezocapacitive sensors with different base structures, and the performance of the sensor with the best performance was tested and the results are

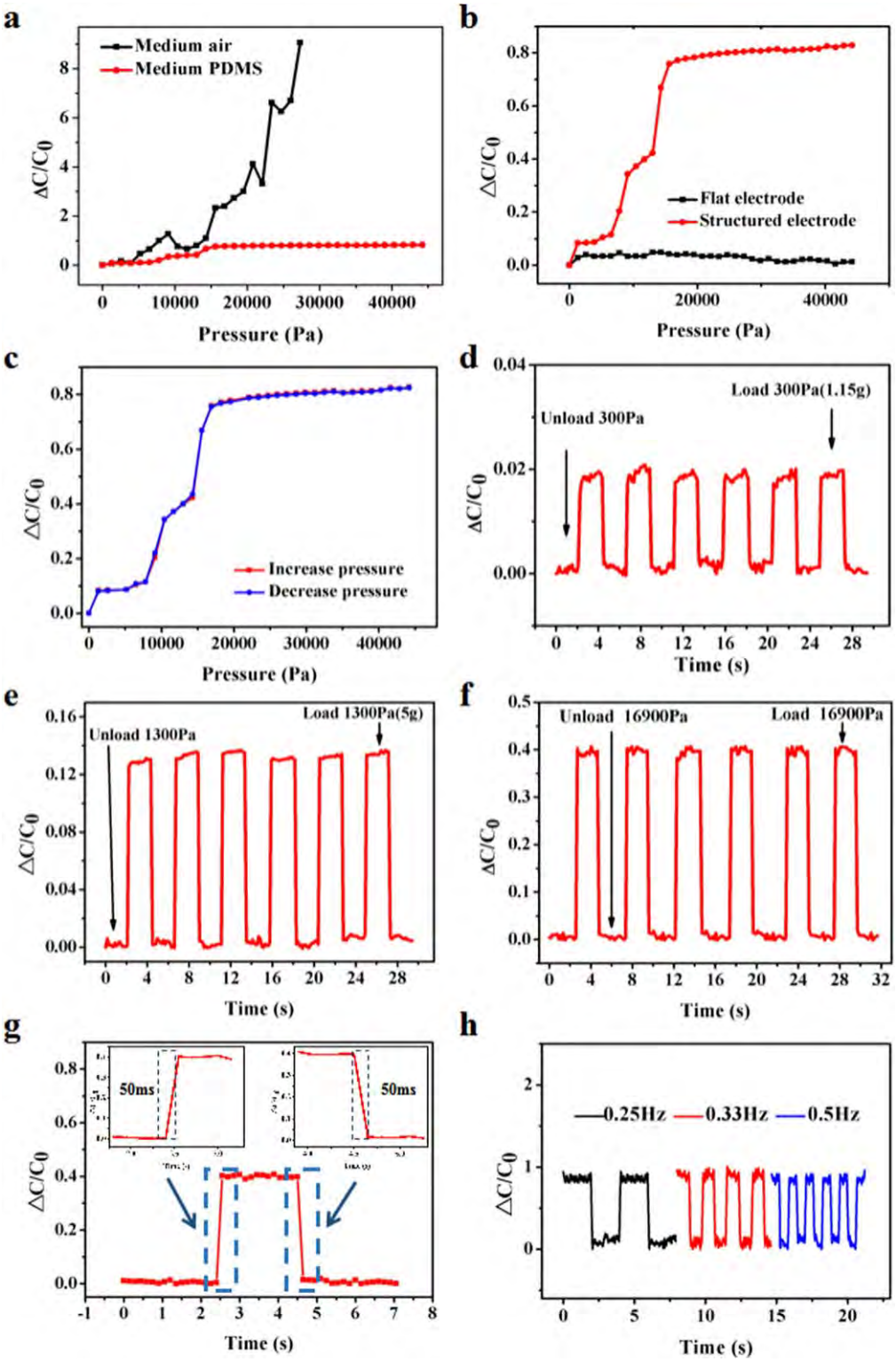

Figure 3. Pressure characteristics of a capacitive pressure sensor.

shown in figure 3. The capacitance value without external pressure is considered to be the initial capacitance C_0, and the capacitance of the pressure sensor to apply pressure is considered to be C. And as a function of the applied pressure (p), a relative capacitance change is plotted [38]

$$\Delta C/C_0 = (C - C_0)/C_0. \tag{1}$$

The slope of the relative capacitance change pressure curve represents the pressure sensitivity [38]

$$S = \delta(\Delta C/C_0)/\delta p. \quad (2)$$

Figure 3(a) shows the pressure test of two different intermediate medium capacitive pressure sensors. It can be seen that the pressure change rate of the air medium pressure sensor is significantly higher than that of the medium PDMS, this is because the sensor of the air medium is more deformed during the application of pressure than the sensor of the PDMS, resulting in a larger change in the distance d between the upper and lower electrodes. However, since the medium is air, the electrode rebounding ability after applying pressure causes the change in capacitance to be extremely unstable and fluctuating. so we chose a capacitive pressure sensor with PDMS as the electrolyte. Figure 3(b) shows the pressure test results of two substrates with different structures (the intermediate medium of both sensors is PDMS). As can be seen from the curve, the change in the capacitance of the upper substrate molded with micropore PE tape is significantly higher than that of the upper substrate molded with glass. And the change in the capacitance of the upper substrate molded with the glass is essentially unchanged. Therefore, we conducted in-depth performance tests on the microstructured capacitive pressure sensor with PDMS as the intermediate medium. Figure 3(c) is a test of sensor loading and unloading. As can be seen from the figure, the loading and unloading curves are substantially coincident, indicating that the sensor changes are stable during the period of pressurization and depressurization. In addition, the sensitivity of the sensor can be divided into two parts (0–15 601 Pa and 15 601–44 202 Pa). When the pressure range is 0–15 601 Pa, $\Delta C/C_0$ is 0.0486 kpa^{-1}. When the pressure range is 15 601–44 202 Pa, $\Delta C/C_0$ is 0.0025 kpa^{-1}. We found that the sensitivity of the sensor is significantly reduced after the applied pressure is increased to 15 601 Pa. The reason for this phenomenon is that the structure of the upper substrate will undergo a huge deformation and the distance between the upper and lower substrates will change significantly due to the higher Young's modulus of PDMS when the lower pressure is applied, which will greatly affect the change of the output capacitance. As the applied pressure increases (pressure is greater than 15 601 Pa), the structure of the upper substrate contact approaches the plane, and the elasticity of the dielectric PDMS is almost close to the limit so that little deformation occurs, resulting in the contact area of the upper substrate is no longer changed and the rate of change of the distance between the upper and lower substrates is reduced, thereby the sensitivity of the sensor is significantly reduced. Figures 3(d)–(f) are repeatability tests for the sensor. Figure 3(d) shows the repeatability test of the sensor under external pressure of 300 Pa. It can be seen that the $\Delta C/C_0$ of the sensor is maintained between 0.017 and 0.022 after the pressure of 300 Pa is applied, and the $\Delta C/C_0$ of the capacitance returns to near zero when the pressure is removed. When repeatedly loading and unloading higher pressures, as shown in figures 3(e) and (f), the $\Delta C/C_0$ output is stable. Figure 3(g) is an enlarged view of a cycle of figure 3(f), from

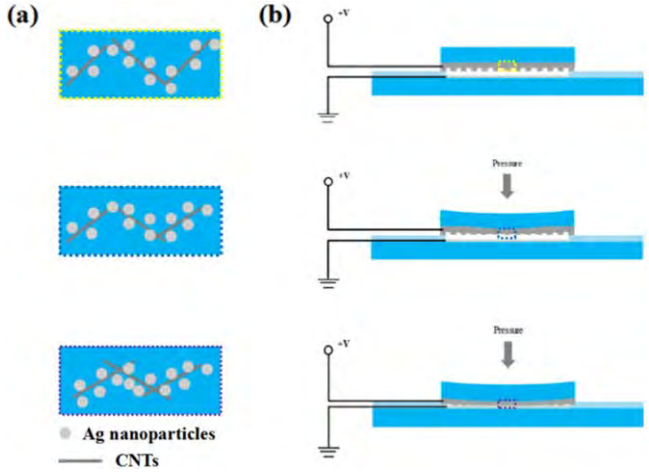

Figure 4. Sensing mechanism of capacitive pressure sensor.

which it can be seen that the response time of the sensor does not exceed 50 ms. Figure 3(h) shows the rate of change of capacitance under the action of different frequencies of the same external force (40 kpa). It can be seen that the test rate result of changing the applied external force will also change steadily.

The sensing mechanism of the piezocapacitive flexible sensor based on the microstructured electrode when subjected to external pressure is shown in figure 4. In general, a capacitor is a structure in which a dielectric is sandwiched between two parallel plates. The capacitance (C) is given by

$$C = \varepsilon_0 \varepsilon_r A/d, \quad (3)$$

where ε_0 is the free space dielectric constant, ε_r is the relative static dielectric constant of the dielectric layer between two parallel plates, A is the overlap area of the two plates, and d is the distance between two plates [49]. In this equation, ε_0 is a constant, and the remaining three variables (ε_r, A, and d) play a crucial role in the capacitance change of the capacitor. The change in ε_r usually be detected by using specially designed materials, and the change in d is always used to measure normal force, shear force and strain. The interpretation of the sensor's sensing mechanism produced in this paper can be summarized in the following four points. First of all, Ag has excellent electrical conductivity and CNTs have good mechanical properties, and the combination of the two can exert their respective advantages, so that the fabricated sensor has better mechanical properties on the basis of good electrical conductivity, thereby the sensor has a wide detection range. Secondly, from the spatial dimension, Ag@CNTs with pore structure is a combination of two spatial dimensions, which increases the roughness of the electrodes and the gaps between the materials themselves, thus broadening the detection range. Thirdly, as mentioned in the above description, since the upper electrode has a special structure, the degree of change is higher than that of the plane by applying the pressure structure, thereby achieving sensitivity superior to that of the sensor having the planar upper electrode. Finally, PDMS as a dielectric layer improves the stability of the sensor, which is derived from figures 3(a) and (c). We

Table 1. Comparison of sensors detection range.

	Sensitive material	Dielectric	Range	References
1	Graphene	PDMS	0–4 kpa	[50]
2	AgNWs	Polymethylmethacrylate (PMMA) or PVP	0–4.5 kpa	[51]
3	AgNWs	Polyvinylidene fluoride (PVDF)	0–7.5 kpa	[17]
4	Pencil	Elastomer	0–30 kpa	[52]
5	Ag@CNTs, AgNWs	PDMS	0–45 kpa	This work
6	AgNPs	PDMS	0–50 kpa	[53]

compared the detection range of some previously published sensors, indicating that the sensor detection range reported in this work is relatively wide, as shown in table 1. The sensor sensing mechanism we produced is shown in figure 4. The sensitive material of the substrate on the sensor is subjected to microscopic changes in pressure as shown in figure 4(a). The dark gray lines in the figure indicate CNTs, and the light gray circles indicate Ag particles. It can be observed that the interaction between Ag@CNTs increases as the external pressure increases, and the continuous shortening of the distance between the upper and lower layers contributes to the increase of capacitance. The side view of the sensor when pressure is applied is shown in figure 4(b). The upper substrate of the sensor has obvious texture and no deformation when no pressure is applied. The middle is the dielectric PDMS and the sensor has an initial capacitance. The upper substrate of the sensor is bent downward by the pressure when the external pressure applies to it, then the upper substrate and the dielectric PDMS are deformed by the extrusion, so that the contact area (A) of the upper substrate changes and the distance (d) between the upper substrate and lower substrate also become shorter, resulting in the output capacitance of the sensor changes. Continue to increase the pressure, due to the over-extrusion resulting in the smaller deformation of sensor, the rate of change of the capacitance becomes smaller until the capacitance is basically no longer changed, which is the maximum detection of the sensor.

We have carried out a series of application tests based on the sensing mechanism and test results. First install the sensor around the neck and issued five syllables to test the sensor, then the curves shown in figures 5(b)–(f). We found from the test results that the distance between the two electrode plates of the capacitive sensor would change with the throat movement during the sound production, which causes the output capacitance of the sensor to change. As shown in figures 5(b), (c), the sensor placement area is recessed downward due to the movement of the larynx when the 'do' or 're' syllable is issued, and the muscles on the upper and lower sides of the sensor squeeze the sensor, causing the middle of the sensor to bulge, so that the distance between the sensor plates is increased and the sensor becomes shorter, thereby make the sensor's capacitance output smaller (this process is shown in figure 5(a ii)). As shown in figures 5(d)–(f), the position where the sensor is placed is bulged when one of these syllables is issued, the sensor is stretched, so that the distance between the two plates of the sensor is reduced and the sensor to become longer, thereby the output capacitance of the sensor is increased (this process is shown in figure 5(a iii)). From the above analysis, we conclude that the direction of motion caused by the vocal cord vibration affects the sensor's capacitance change when different syllables are emitted. Similarly, the sensor outputs different waveforms through the vocal cord vibration when we say some phrases as shown in figures 5(g)–(j), the black circle marked in the picture is a slight pause when speaking, '∼' means the aftersound at the end of the voice, so we can judge the vibration direction of the vocal cord by the output waveform of the sensor. Through the above tests of voice, this sensor can contribute to the expected change of the phone type function, which will be very interesting. In addition, the sensor can be installed at the wrist to detect the vibration of the pulse as shown in figure 5(k) and the pulse can be calculated by the interval between two systolic peaks, showing an interval of 0.85 s and beats per minute of ∼70. Therefore, Ag@CNTs with special structure are used here as the sensitive material of a substrate on the sensor and the capacitive pressure sensor prepared by micropore PE tape molding was reported to have wide pressure detection range. And the sensor can be applied to identify sound, monitor pulse or array for electronic skin sensing pressure range, etc.

4. Conclusion

In this study, we developed a wide detection limit capacitive pressure sensor based on a structured elastomeric electrode that can be mass-produced in a simple and low cost way. This capacitive pressure sensor exhibits low detection limit (<300 Pa), wide detection range (0–45 kpa), ultra-short response time (<50 ms) and high operational stability for repeated loading/unloading pressure cycles. The structure of the mold by micropore PE tape significantly increases the effective contact area of the electrode and changes the overlap area and the distance between the electrodes under external pressure, showing excellent pressure sensitivity. The sensor owns excellent resolution and can distinguish language. In addition, the sensor can be used to monitor pulse. The pressure sensor can be fabricated in an array to detect the load pressure distribution and intensity. Low-cost mass production and wide detection range of flexible capacitive pressure sensors lay the foundation for the development of electronic skin, contact inspection applications and wearable healthcare monitors.

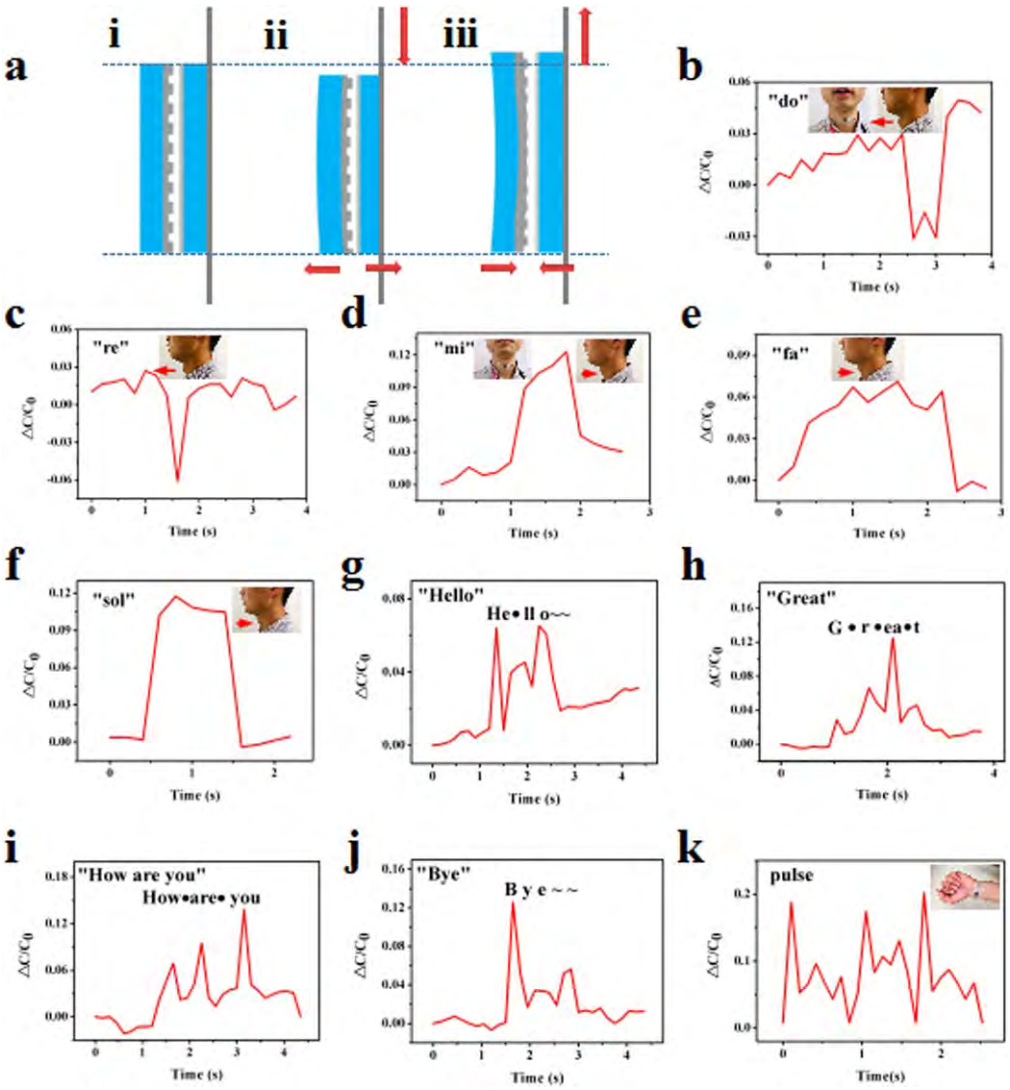

Figure 5. Application testing of capacitive sensors.

Acknowledgments

This study was financially supported by National Natural Science Foundation of China (Nos. 61703298; 51622507; 51705354) Basic Research Program of Shanxi for Youths (Nos. 201701D221110, 201701D221111) and 863 project (2015AA042601).

Notes

The authors declare no competing financial interest.

ORCID iDs

Wendong Zhang https://orcid.org/0000-0001-5997-326X
Shengbo Sang https://orcid.org/0000-0003-4974-9306

References

[1] Chortos A, Liu J and Bao Z 2016 *Nat. Mater.* **15** 937
[2] Lou Z *et al* 2017 *Nano Energy* **38** 28
[3] Mu J, Hou C, Wang G, Wang X, Zhang Q, Li Y, Wang H and Zhu M 2016 *Adv. Mater.* **28** 9491
[4] Tai Y L and Yang Z G 2015 *J. Mater. Chem.* B **3** 5436
[5] Lai Y C, Ye B W, Lu C F, Chen C T, Jao M H, Su W F, Hung W Y, Lin T Y and Chen Y F 2016 *Adv. Funct. Mater.* **26** 1286
[6] Lu N and Kim D-H 2014 *Soft Robot.* **1** 53
[7] Majidi C 2014 *Soft Robot.* **1** 5
[8] Kong J H, Jang N S, Kim S H and Kim J M 2014 *Carbon* **77** 199
[9] Tai Y L, Mulle M, Aguilar Ventura I and Lubineau G A 2015 *Nanoscale* **7** 14766
[10] Choi S, Lee H, Ghaffari R, Hyeon T and Kim D H 2016 *Adv. Mater.* **28** 4203
[11] Jang H, Park Y J, Chen X, Das T, Kim M S and Ahn J H 2016 *Adv. Mater.* **28** 4184
[12] Chen S, Zhuo B and Guo X 2016 *ACS Appl. Mater. Interfaces* **8** 20364
[13] Khan Y, Ostfeld A E, Lochner C M, Pierre A and Arias A C 2016 *Adv. Mater.* **28** 4373

[14] Boutry C M, Nguyen A, Lawal Q O, Chortos A, Rondeau-Gagne S and Bao Z 2015 *Adv. Mater.* **27** 6954
[15] Kwon D, Lee T I, Shim J, Ryu S, Kim M S, Kim S, Kim T S and Park I 2016 *ACS Appl. Mater. Interfaces* **8** 16922
[16] Wang J *et al* 2017 *Nano Energy* **33** 418
[17] Shuai X *et al* 2017 *ACS Appl. Mater. Interfaces* **9** 26314
[18] Yang C, Li L, Zhao J, Wang J, Xie J, Cao Y, Xue M and Lu C 2018 *ACS Appl. Mater. Interfaces* **10** 25811
[19] Yin F, Yang J, Peng H and Yuan W 2018 *J. Mater. Chem.* C **6** 6840
[20] Pang Y, Tian H, Tao L, Li Y, Wang X, Deng N, Yang Y and Ren T-L 2016 *ACS Appl. Mater. Interfaces* **8** 26458
[21] Lee D, Lee H, Jeong Y, Ahn Y, Nam G and Lee Y 2016 *Adv. Mater.* **28** 9364
[22] Song X, Sun T, Yang J, Yu L, Wei D, Fang L, Lu B, Du C and Wei D 2016 *ACS Appl. Mater. Interfaces* **8** 16869
[23] You B, Han C J, Kim Y, Ju B-K and Kim J W 2016 *J. Mater. Chem.* A **4** 10435
[24] Shi R *et al* 2018 *Sci. China Mater.* **61** 1587
[25] Kim H *et al* 2018 *Small* **14** 1703432
[26] Joo Y, Byun J, Seong N, Ha J, Kim H, Kim S, Kim T, Im H, Kim D and Hong Y 2015 *Nanoscale* **7** 6208
[27] Lee K *et al* 2017 *Small* **13** 1700368
[28] Chun J, Lee K Y, Kang C Y, Kim M W, Kim S W and Baik J M 2014 *Adv. Funct. Mater.* **24** 2038
[29] Pan C F, Dong L, Zhu G, Niu S M, Yu R M, Yang Q, Liu Y and Wang Z L 2013 *Nat. Photon.* **7** 752
[30] Persano L, Dagdeviren C, Su Y W, Zhang Y H, Girardo S, Pisignano D, Huang Y G and Rogers J A 2013 *Nat. Commun.* **4** 1633
[31] Lee J H, Yoon H J, Kim T Y, Gupta M K, Lee J H, Seung W, Ryu H and Kim S W 2015 *Adv. Funct. Mater.* **25** 3203
[32] Lin L, Xie Y N, Wang S H, Wu W Z, Niu S M, Wen X N and Wang Z L 2013 *ACS Nano* **7** 8266
[33] Zhang H, Yang Y, Su Y, Chen J, Adams K, Lee S, Hu C and Wnag Z L 2014 *Adv. Funct. Mater.* **24** 1401
[34] Yao S S and Zhu Y 2014 *Nanoscale* **6** 2345
[35] Park S *et al* 2014 *Adv. Mater.* **26** 7324
[36] Zhao X, Hua Q, Yu R, Zhang Y and Pan C 2015 *Adv. Electron. Mater.* **1** 1500142
[37] Sheng L Z, Liang Y, Jiang L L, Wang Q, Wei T, Qu L T and Fan Z J 2015 *Adv. Funct. Mater.* **25** 6545
[38] Wan Y, Wang Y and Guo C F 2017 *Mater. Today Phys.* **1** 61
[39] Huang Y *et al* 2019 *Adv. Funct. Mater.* **29** 1808509
[40] Bao R *et al* 2015 *Adv. Funct. Mater.* **25** 2884
[41] Jian M *et al* 2017 *Adv. Funct. Mater.* **27** 1606066
[42] Zhou J *et al* 2016 *Nanoscale* **9** 604
[43] Hoang P T *et al* 2016 *Nanoscale Res. Lett.* **11** 422
[44] Zhang Q *et al* 2017 *Nanomaterials* **7** 424
[45] Zhang K, Du Y and Chen S 2015 *Org. Electron.* **26** 380
[46] Wang X *et al* 2014 *Adv. Mater.* **26** 1309
[47] Li T *et al* 2016 *Small* **12** 5042
[48] Chun J *et al* 2014 *Adv. Funct. Mater.* **24** 2038
[49] Hammock M L, Chortos A, Tee B C K, Tok J B H and Bao Z 2013 *Adv. Mater.* **25** 5997e6037
[50] Yang J *et al* 2019 *ACS Appl. Mater. Interfaces* **11** 14997
[51] Joo Y *et al* 2015 *Nanoscale* **7** 6208
[52] Lee K *et al* 2017 *Small* **13** 1700368
[53] Chhetry A, Yoon H and Park J Y *J. Mater. Chem.* C **5** 10068